JVI Journals.ASM.org

The Essential, Nonredundant Roles of RIG-I and MDA5 in Detecting and Controlling West Nile Virus Infection

John S. Errett,[a] Mehul S. Suthar,[b] Aimee McMillan,[a] Michael S. Diamond,[c] Michael Gale, Jr.[a]

Department of Immunology, University of Washington School of Medicine, Seattle, Washington, USA[a]; Department of Pediatrics, Emory Vaccine Center at Yerkes, Emory University, Atlanta, Georgia, USA[b]; Departments of Medicine, Molecular Microbiology, and Pathology and Immunology, Washington University School of Medicine, St. Louis, Missouri, USA[c]

Virus recognition and response by the innate immune system are critical components of host defense against infection. Activation of cell-intrinsic immunity and optimal priming of adaptive immunity against West Nile virus (WNV), an emerging vector-borne virus, depend on recognition by RIG-I and MDA5, two cytosolic pattern recognition receptors (PRRs) of the RIG-I-like receptor (RLR) protein family that recognize viral RNA and activate defense programs that suppress infection. We evaluated the individual functions of RIG-I and MDA5 both *in vitro* and *in vivo* in pathogen recognition and control of WNV. Lack of RIG-I or MDA5 alone results in decreased innate immune signaling and virus control in primary cells *in vitro* and increased mortality in mice. We also generated *RIG-I*$^{-/-}$ × *MDA5*$^{-/-}$ double-knockout mice and found that a lack of both RLRs results in a complete absence of innate immune gene induction in target cells of WNV infection and a severe pathogenesis during infection *in vivo*, similar to findings for animals lacking MAVS, the central adaptor molecule for RLR signaling. We also found that RNA products from WNV-infected cells but not incoming virion RNA display at least two distinct pathogen-associated molecular patterns (PAMPs) containing 5′ triphosphate and double-stranded RNA that are temporally distributed and sensed by RIG-I and MDA5 during infection. Thus, RIG-I and MDA5 are essential PRRs that recognize distinct PAMPs that accumulate during WNV replication. Collectively, these experiments highlight the necessity and function of multiple related, cytoplasmic host sensors in orchestrating an effective immune response against an acute viral infection.

West Nile virus (WNV) is a positive-sense single-stranded RNA (ssRNA) virus of the flavivirus genus and has recently emerged as a primary cause of viral encephalitis in the Western hemisphere (1). The virus was endemic originally to portions of Africa and Asia, where it cycles in nature between birds and mosquitoes. Humans become infected with WNV as incidental hosts following virus exposure from a feeding, infected mosquito. Since its emergence into North America in 1999, there have been over 36,000 cases of human WNV infection in the United States, including the second highest annual peak of over 5,000 cases in 2012 alone (2, 3). Moreover, there remains a potential for newly emerging pathogenic WNV strains to cause additional and possibly increasingly severe human outbreaks (4, 5). Infection with WNV is characterized by an acute febrile episode that can progress to neuroinvasive disease, including encephalitis, meningitis, and flaccid paralysis. The greatest risk for severe disease is in the elderly and immunocompromised (6). In human WNV cases with neuroinvasive disease, death occurs in approximately 10% of patients (1, 2, 7, 8).

Many aspects of WNV infection, immunity, and clinical disease in humans are recapitulated in mouse challenge models. Subcutaneous inoculation of WNV in mice results in a pathogenesis sequence that includes local infection in cells (keratinocytes and Langerhans cells) of the skin, migration of infected dendritic cells to the draining lymph nodes, and the development of viremia, which ultimately facilitates crossing of the blood-brain barrier and infection of neurons in the central nervous system (CNS) (7, 9). The mouse model of WNV infection has revealed many key host-pathogen interactions that control the outcome of WNV infection and immunity (7, 10). Components of the innate and adaptive immune system are essential for protection from WNV infection. Innate immune programs involved in pathogen recognition, signal transduction, and effector function are required for effective antiviral immunity against WNV infection and disease (11–19), whereas antibody and cell-mediated immunity is necessary for limiting virus dissemination, clearing WNV from target cells in the periphery and CNS, and preventing disease after secondary exposure (20–22). An underlying concept extending from many studies of WNV infection in gene knockout (KO) mice is that compromise of innate antiviral immunity can ultimately result in enhancement of virus entry or replication in the CNS, leading to neurologic disease and mortality (10).

During WNV infection, the innate immune response serves to control tissue tropism of infection and restrict virus entry into the CNS (10, 23, 24). WNV and other RNA viruses trigger the innate host defense response upon non-self recognition by the RIG-I-like receptors (RLRs), including RIG-I and melanoma differentiation antigen 5 (MDA5) (25). Prior studies in cell culture have shown that flavivirus recognition during acute infection is mediated by both RIG-I and MDA5 (26). For WNV, the RLRs are required for induction of type I interferon (IFN) and innate antiviral responses, with RIG-I proposed to induce gene expression early in infection and MDA5 signaling occurring at a later stage (12, 14, 27, 28). RLR signaling is mediated through the adaptor protein MAVS, which itself is essential for controlling WNV infection and immunity *in vitro* and *in vivo* (14). MAVS-dependent RLR signal-

Received 3 June 2013 Accepted 12 August 2013
Published ahead of print 21 August 2013
Address correspondence to Michael Gale, Jr., mgale@u.washington.edu.

doi:10.1128/JVI.01488-13

ing activates the transcription factors IFN regulatory factor 3 (IRF-3), IRF-5, IRF-7, and NF-κB, to promote gene expression programs that limit WNV replication and spread and to modulate adaptive immunity (16, 17, 27, 29–31).

RIG-I is believed to bind to WNV RNA to initiate innate immune signaling, but the specific determinants of recognition of flavivirus RNA by RIG-I remain unknown (32). Moreover, the role of MDA5 in WNV recognition is not well defined, nor have the combinatorial and distinct functions of RIG-I and MDA5 in pathogen recognition and host defense been revealed. Studies that characterize pathogen-associated molecular pattern (PAMP) ligands of RIG-I have demonstrated that non-self recognition depends on several properties of viral RNA, including PAMP motif length, structure, modification, and composition (33–36). Multiple studies show that RNA ligands of RIG-I require an exposed 5′ triphosphate (5′-ppp) for recognition and binding (33, 35, 37). Studies to characterize the features of an MDA5-specific PAMP ligand show that long, stable double-stranded RNA (dsRNA) and/or "higher order" RNA complexes containing both dsRNA and ssRNA are preferred PAMP ligands, though the nature of such RNA complexes is unknown (38, 39). The ~11-kb WNV genome contains a 5′ Cap-1 structure that is expected to mask the 5′-ppp necessary for RIG-I recognition. The dsRNA replication intermediates or highly structured subgenomic fragments that accumulate within cells during infection could serve as possible MDA5 ligands (7, 40), although such PAMPs may be sequestered in membrane-derived replication "packets" with limited accessibility to RLRs (41, 42). As flaviviruses share a replication program (43), assessment of WNV interactions with RIG-I and MDA5 will provide a general understanding of how the host recognizes cellular infection by flaviviruses, which include a family of related pathogens of global public health concern such as dengue virus (26), Japanese encephalitis virus (44), and yellow fever virus (45).

In the current study, we assessed the individual and combined roles of RIG-I and MDA5 in pathogen recognition and immunity to WNV infection using wild-type (WT) and RLR KO mice and cells. We show that each RLR individually contributes to pathogen recognition and immune protection against WNV *in vivo* and *in vitro*, and we establish that RIG-I and MDA5 detect distinct PAMPs with differential kinetics during the course of WNV replication to mediate complementary, nonredundant roles in viral detection and innate immune gene induction.

MATERIALS AND METHODS

Mouse studies. *RIG-I*$^{-/-}$ mice and their wild-type littermate controls have been described previously (44, 46) and were obtained as a generous gift from S. Akira (Osaka University). *MDA5*$^{-/-}$ mice were kindly provided by M. Colonna (Washington University, St. Louis, MO). *MAVS*$^{-/-}$ mice were previously described (47). For production of double knockout (DKO) mice lacking both *RIG-I* and *MDA5*, *RIG-I*$^{-/-}$ and *MDA5*$^{-/-}$ mice were intercrossed, and the resulting DKO offspring were backcrossed into a C57BL/6 background through the F3 generation. The resulting DKO line used in this study has an approximately 94% C57BL/6 genetic background, as determined by microsatellite DNA analysis. All mice were genotyped and bred under pathogen-free conditions in the animal facility at the University of Washington. Experiments were performed with approval from the University of Washington Institutional Animal Care and Use Committee. Age-matched 6- to 12-week-old mice were inoculated subcutaneously (s.c.) in the left rear footpad with 100 PFU of WNV isolate TX 2002-HC (WNV-TX) in a 10-μl inoculum diluted in Hanks balanced salt solution (HBSS) supplemented with 1% heat-inactivated fetal bovine serum (FBS). Mice were monitored daily for morbidity and mortality.

Cells and viruses. Working stocks of WNV-TX were generated by propagation on Vero E6 cells, and titers were determined by standard plaque assay on BHK-21 cells as previously described (14). This virus preparation and methods differ slightly from those used for WNV-NY in the study described in the accompanying paper by Lazear et al. (48). WNV infections were performed by incubating virus at the indicated multiplicity of infection (MOI) with cells in serum-free medium for 1 h, followed by removal of the virus and addition of Dulbecco modified Eagle medium (DMEM) supplemented with 10% FBS, 1 mM sodium pyruvate, 2 mM L-glutamine, 1× HEPES (pH 7.3), antibiotic-antimycotic solution, and 1× nonessential amino acids (complete DMEM). Primary mouse embryonic fibroblasts (MEFs) were generated from *RIG-I*$^{-/-}$, *MDA5*$^{-/-}$, *MAVS*$^{-/-}$, *RIG-I*$^{-/-}$ × *MDA5*$^{-/-}$ DKO, and WT control mice as previously described (17) and grown in complete DMEM. To facilitate direct comparison of signaling in our PAMP characterization studies, we also generated primary MEFs from *RIG-I*$^{-/-}$ embryos of the F3 generation backcrossed onto the C57BL/6 background and used these cells to compare directly to WT, *MDA5*$^{-/-}$, and DKO MEFs. Primary bone marrow-derived macrophages (Mϕ) and dendritic cells (DCs) were generated as described previously (17). Sendai virus, Cantell strain, was purchased from Charles River. Cells were infected with 100 HA units per ml of Sendai virus and harvested at 24 h postinfection. Encephalomyocarditis virus (ECMV) was a gift of R. Silverman (Cleveland Clinic), and cells were infected at an MOI of 5 and harvested at 24 h postinfection.

IFN-β ELISA. IFN-β in cell culture supernatants was measured by using the mouse-specific IFN-β enzyme-linked immunosorbent assay (ELISA) kit according to the manufacturer's protocol (PBL Biomedical Laboratories).

RNA extraction and analysis. Total cellular RNA from cultured cells was collected for quantitative reverse transcription-PCR (qRT-PCR) using the RNeasy kit (Qiagen) and reverse transcribed using the iScript select cDNA synthesis kit using both oligo(dT) and random primers (Bio-Rad). Cellular mRNA and viral RNA expression levels were determined by SYBR green qRT-PCR using gene- or virus-specfic primers. Specific primer sets are as follows: mGAPDH forward, CAACTACATGGTCTAC ATGTTC; mGAPDH reverse, CTCGCTCCTGGAAGATG; mIFNβ forward, GGAGATGACGGAGAAGATGC; mIFNβ reverse, CCCAGTGCT GGAGAAATTGT; mIL6 forward, GTTCTCTGGGAAATCGTGGA; mIL6 reverse, TGTACTCCAGGTAGCTATGG; WNV forward, CGCCT GTGTGAGCTGACAAAC; WNV reverse, CATAGCCCTCTTCAGTCC; mIFN-a2a, purchased from SA Biosciences; mIRF-7 forward, CCCATCT TCGACTTCAGCAC; mIRF-7 reverse, TGTAGTGTGGTGACCCTTGC; mIFIT2 forward, CTGGGGAAACTATGCTTGGGT; and mIFIT2 reverse, ACTCTCTCGTTTTGGTTCTTGG.

RNA preparation. Infected cell RNA (icRNA) or mock-infected cell RNA (mcRNA) was extracted using TRIzol LS reagent according to the manufacturer's protocol (Invitrogen). WNV virus particle RNA (virion RNA) was purified by layering precleared infected cell supernatants over a 20% sucrose cushion, followed by centrifugation for 4 h at 70,000 × *g* in a Beckman Coulter SW 40 Ti rotor. RNA was extracted from sedimented virions using TRIzol LS. *In vitro*-transcribed 5′ and 3′ nontranslated regions (NTR) of WNV were generated as previously described (40, 49). RNA concentrations were determined by absorbance using a NanoDrop spectrophotometer. icRNA was treated with Antarctic phosphatase (AP) to remove phosphate moieties or RNase III to digest dsRNA, followed by ethanol and sodium acetate precipitation (New England BioLabs). Transfections of RNA were performed with a TransIT-mRNA transfection kit according to the manufacturer's protocol (Mirus Bio) into cells pretreated for 30 min with 20 μg/ml of cycloheximide (CHX) in complete DMEM. Total cellular RNA from transfected cells was collected for qRT-PCR 8 to 10 h posttransfection using an RNeasy kit.

Immunoblot analysis. Protein extracts were prepared as previously described (50), and 20 μg of protein lysate was analyzed by SDS-poly-

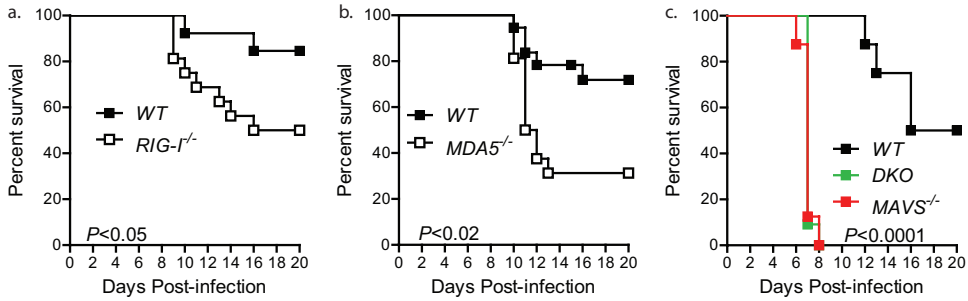

FIG 1 *In vivo* pathogenesis of RLR KO mice infected with WNV. Adult RLR KO mice and WT controls were infected with 10^2 PFU of WNV and monitored for survival. *RIG-I*$^{+/+}$ mixed-background mice ($n = 13$) and *RIG-I*$^{-/-}$ mixed-background mice ($n = 16$) (a), C57BL/6 WT ($n = 37$) and *MDA5*$^{-/-}$ mice ($n = 16$) (b), and *RIG-I*$^{-/-}$ × *MDA5*$^{-/-}$ ($n = 11$) mice, *RIG-I*$^{+/+}$ × *MDA5*$^{+/+}$ littermate controls ($n = 8$), and *MAVS*$^{-/-}$ ($n = 8$) mice (c) all exhibit significantly greater mortality rates than did their respective controls ($P < 0.05$, $P < 0.02$, and $P < 0.0001$).

acrylamide gel electrophoresis followed by immunoblotting. The following primary antibodies were used: anti-murine IFIT2 (gift of G. Sen, Cleveland Clinic), goat anti-WNV NS3 (R&D Systems), mouse antitubulin (Sigma), and mouse anti-glyceraldehyde-3-phosphate dehydrogenase (anti-GAPDH; Santa Cruz). All secondary antibodies were purchased from Jackson ImmunoResearch. Immunoreactive bands were detected with Amersham ECL Plus reagent (GE Healthcare).

Statistical analysis. *In vivo* Kaplan-Meier curves were analyzed by log rank test. All *in vitro* statistics were obtained by an unpaired, two-tailed Student *t* test. A *P* value of <0.05 was considered significant. All data were analyzed using Prism software (GraphPad Prism).

RESULTS

RIG-I and MDA5 are essential for protection against WNV infection *in vivo*. To determine the individual roles of RIG-I and MDA5 in WNV infection and immunity, we assessed WNV pathogenesis in WT mice and in *RIG-I*$^{-/-}$ or *MDA5*$^{-/-}$ mice. An in-depth, direct analysis of the respective roles of the individual RLRs has been hampered by the embryonic lethality of the *RIG-I*$^{-/-}$ genotype in a complete C57BL/6 background, while *MDA5*$^{-/-}$ mice are fully viable on several genetic backgrounds (44). To circumvent embryonic lethality, the *RIG-I*$^{+/+}$and *RIG-I*$^{-/-}$ mice were generated on a mixed ICR × 129Sv × C57BL/6 genetic background (44). *MDA5*$^{-/-}$ mice, in comparison, were generated originally on a 129Sv background without any noted developmental defects (51) and were backcrossed subsequently to a 99% pure C57BL/6 background to facilitate WNV pathogenesis studies. Each RLR single-knockout mouse line was evaluated in comparison to its own individual wild-type (WT) control. We infected mice subcutaneously with 10^2 PFU of WNV-TX and monitored morbidity and mortality. *RIG-I*$^{-/-}$ mice were more susceptible to WNV infection than were their WT controls, with enhanced lethality (50% versus 17%, $P < 0.05$) observed over the 20-day monitoring period of infection (Fig. 1a). Similar results were obtained when we compared *MDA5*$^{-/-}$ mice with their respective WT controls, with significantly more (70% versus 30%; $P < 0.02$) *MDA5*$^{-/-}$ mice dying from WNV infection (Fig. 1b). We also intercrossed *RIG-I*$^{-/-}$ × *MDA5*$^{-/-}$ double-knockout (DKO) mice lacking expression of both RIG-I and MDA5, and this line was backcrossed into a C57BL/6 background through the F3 generation to yield a strain of ~94% C57BL/6, as defined by microsatellite DNA analysis (data not shown). DKO mice exhibited markedly increased susceptibility to WNV infection compared to that of WT C57BL/6 control mice or *RIG-I*$^{-/-}$ or *MDA5*$^{-/-}$ mice, and they had a more rapid mean time to death, ~8 days (100% versus 50%; $P < 0.0001$) (Fig. 1c). The susceptibility of DKO mice to WNV infection was remarkably similar to that of *MAVS*$^{-/-}$ mice, which were generated on a pure C57BL/6 background (Fig. 1c) (14). These results demonstrate that RLR signaling from both RIG-I and MDA5 is required for protection against WNV infection *in vivo*.

RIG-I and MDA5 are both required for innate immune gene induction and control of WNV replication. To determine how RIG-I and MDA5 individually regulate innate immune gene expression and control of WNV replication, we performed a detailed time course analysis of gene expression and virus replication within low-passage-number primary MEFs from *RIG-I*$^{+/+}$ WT, *RIG-I*$^{-/-}$, C57BL/6 WT, *MDA5*$^{-/-}$, and DKO mice. For each analysis, we measured viral RNA and compared innate immune gene expression in mock-infected cells with that in WNV-infected cells at a high multiplicity of infection (MOI = 5), determining the fold change in RNA expression levels (Fig. 2). Whereas WNV RNA replicated to higher levels (4-fold difference [$P < 0.003$] at 48 h postinfection [hpi]) throughout the 48-h time course in *RIG-I*$^{-/-}$ than in cognate WT MEFs (Fig. 2a), no appreciable differences in viral infection were observed between WT and *MDA5*$^{-/-}$ cells ($P > 0.05$ at 48 hpi) (Fig. 2b). The IFN-β gene is an acute innate immune response gene that is induced early after virus infection (10). The increase in WNV replication in *RIG-I*$^{-/-}$ MEFs corresponded with an early deficit (14- and 13-fold differences [$P < 0.03$] at 8 and 10 hpi) of IFN-β mRNA induction, with expression reaching WT levels subsequently (Fig. 2c). In comparison, IFN-β expression was induced equivalently in WNV-infected WT and *MDA5*$^{-/-}$ cells throughout the time course ($P > 0.05$ at 10 and 48 hpi) (Fig. 2d). We also examined the WNV-induced expression of the gene for IFN-α2a, a comparably late-expressed innate immune response cytokine that amplifies and diversifies innate immune gene expression. IFN-α2a is induced after IFN-β signaling, as it requires IRF-7 induction and activation (17, 52). We failed to detect a major difference in IFN-α2a mRNA expression over a course of 22 to 48 hpi between WT and *RIG-I*$^{-/-}$ cells (Fig. 2e). Remarkably, *MDA5*$^{-/-}$ cells showed a significant deficit in IFN-α2a expression (2- and 3.8-fold differences [$P < 0.003$] at 34 and 42 hpi, respectively) compared to WT controls at late time points of infection (Fig. 2f). These results verify that RIG-I is essential for early innate immune gene induction and virus control (12) and reveal a specific role for MDA5 in the later, amplification phase of the innate immune response after

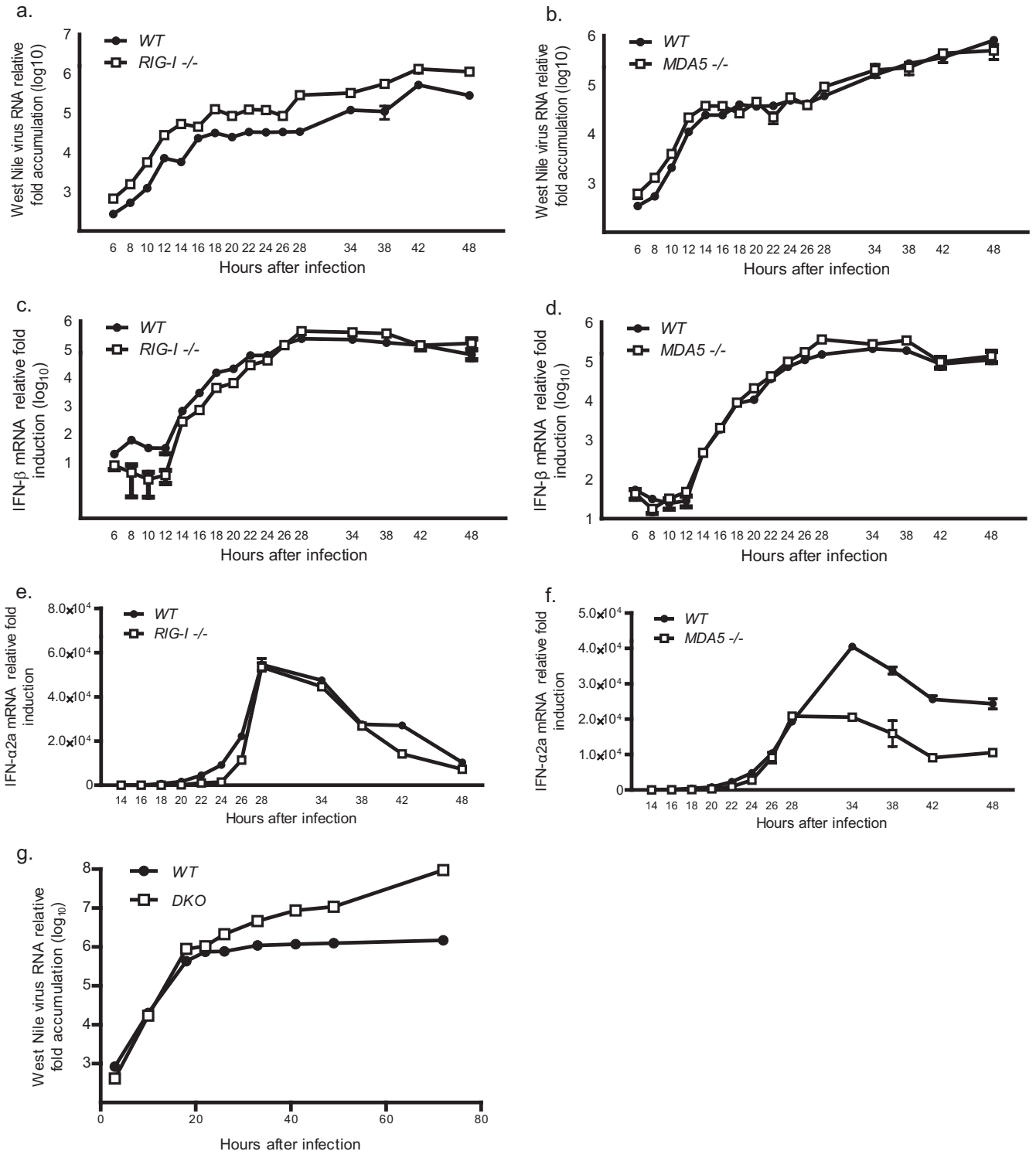

FIG 2 Innate immune gene expression and viral RNA accumulation over a WNV infection time course. Primary MEFs were infected with WNV or mock infected, and innate immune gene induction or viral RNA accumulation in each cell line was determined by qRT-PCR and plotted as relative fold induction compared to that of mock cells and normalized to GAPDH expression. Cell lines used for panels a to f were mixed-background *RIG-I*$^{+/+}$ or *RIG-I*$^{-/-}$ compared to each other or C57BL/6 WT and *MDA5*$^{-/-}$ compared to each other. Panels a and b, c and d, and e and f represent WNV RNA, IFN-β mRNA, and IFN-α2a mRNA accumulation over time in infected MEFs. The graphs show the means ± SDs from triplicate analyses and are representative of three independent experiments. (g) WNV RNA accumulation in WT versus *RIG-I*$^{-/-}$ × *MDA5*$^{-/-}$ MEFs; a summary of innate immune gene induction is shown in Table 1.

TABLE 1 RLR-induced innate immune genes[a]

Gene	Fold induction in cell type	
	WT	DKO
IFIT2	146.1	1.7
IL-6	36.6	0.6
IFN-α2a	467.6	0.9
IRF-7	804.5	2.0
IFN-β	32,294.5	2.5

[a] Summary of the innate immune gene induction from WT and DKO cells infected with WNV and plotted in Fig. 2g. All genes were RIG-I dependent early and MDA5 dependent late. Values represent the fold induction at the peak of the innate immune response from the time course infection in Fig. 2g.

WNV infection. We note that the early deficit in IFN-β production resulted in increased viral replication in infected cells during time points before WNV can efficiently antagonize IFN signaling, whereas the late defect in IFN-α2a production did not result in increased WNV replication in MEFs under single-step growth kinetic conditions, possibly because at these points accumulated viral nonstructural proteins can antagonize IFN signaling (53, 54).

We next assessed the combined roles of RIG-I and MDA5 in controlling WNV replication and promoting innate immune gene induction in MEFs. DKO cells were mock infected or infected with WNV over a 72-h time course. As expected, WNV RNA accumulated to much higher levels (>60-fold difference at 72 hpi) in DKO than in WT cells (Fig. 2g). We also performed qRT-PCR analysis to examine the expression of a subset of RLR-responsive innate immune genes previously identified from transcriptional profiling studies of WNV-infected cells (12). Remarkably, while these genes were induced highly in WT cells, none were significantly induced in DKO cells after WNV infection (Table 1). These observations are consistent with recent results demonstrating that in target cells of WNV infection, MAVS-dependent signaling is the predominant pathway through which viral RNA is sensed for host defense gene induction (29). Our results demonstrate that RIG-I and MDA5 are the two essential PRRs that sense WNV infection and induce the antiviral response through MAVS-dependent signaling.

MDA5 is required to control virus replication in myeloid cells. Our results suggest that RIG-I mediates early/initial PAMP recognition and signaling, while MDA5 mediates late signaling to amplify innate immune actions during WNV infection. While previous studies support a role for RIG-I in initial triggering of innate immune defenses against WNV infection, the role of MDA5 in this process has not been evaluated (12, 28, 32). To assess the role of MDA5 in innate immune signaling in bona fide *in vivo* target cells of WNV infection, we performed time course analysis to evaluate the levels of infectious WNV production and gene induction in primary bone marrow-derived macrophages (Mϕ) and dendritic cells (DCs) prepared from WT and $MDA5^{-/-}$ mice. Mϕ and DCs from $MDA5^{-/-}$ mice supported increased virus growth compared to WT cells (4-fold difference [$P < 0.04$] at 36 h and 2- and 3-fold differences [$P < 0.008$ and $P < 0.02$], respectively) (Fig. 3a and b). Immunoblot analysis demonstrated that WNV proteins accumulated to higher levels in $MDA5^{-/-}$ Mϕ and DCs than in WT cells (especially at 36 h), whereas DCs exhibited a concomitant reduction in the virus-induced expression of IFIT2, an IFN-stimulated gene (ISG) that is downstream of RLR signaling and restricts WNV infection (Fig. 3c and d) (50, 55). We also found that $MDA5^{-/-}$ Mϕ and DCs produced lower levels of IFN-β postinfection than WT cells (Fig. 3e and f), despite the increased viral burden. As controls, we also assessed IFN-β production in response to Sendai virus (a RIG-I-specific stimulus [44]) and encephalomyocarditis virus (ECMV; an MDA5-specific stimulus [51]), respectively, in WT and $MDA5^{-/-}$ Mϕ and DCs. Although Sendai virus induced robust production of IFN-β, ECMV infection failed to induce IFN-β production in $MDA5^{-/-}$ DCs. These results demonstrate that MDA5 is essential for optimal control of WNV replication and induction of antiviral host defense genes in cells that are targets of infection *in vivo*.

To assess the combined roles of RIG-I and MDA5 in detecting and controlling WNV infection in myeloid cells, we generated DKO DCs and compared their response with those of WT and $MAVS^{-/-}$ cells. WNV replicated to increased levels (18-fold higher) in DKO cells compared to WT cells, similar to observations in parallel cultures of $MAVS^{-/-}$ DCs (17-fold higher) (Fig. 3g). Moreover, and in contrast to $MDA5^{-/-}$ cells, there was no detectable induction of IFN-β production or innate immune gene expression (compare Fig. 3a to d with Fig. 3h and i) by DKO or $MAVS^{-/-}$ DCs after WNV infection. Thus, while MDA5 is required for optimal innate immune gene induction and control of WNV infection, in myeloid cells the combination of RIG-I and MDA5 and subsequent signaling through MAVS is essential for WNV detection and innate immune gene induction.

WNV PAMP characteristics for RLR detection. To determine the properties of the PAMPs that trigger RLR signaling during WNV infection, we examined the signaling actions of RNA recovered from mock-infected control cells (mcRNA), cells infected with WNV for 24 h (icRNA), specific WNV RNA secondary-structure motifs, and native virion RNA when transfected into primary MEFs. We first purified RNA from mock- and WNV-infected cells to generate control mcRNA and icRNA. mcRNA transfection induces only very low IFN-β mRNA levels, and we thus normalized all data sets against the response to mcRNA (Fig. 4a). RNA also was obtained from WNV virions (vRNA) by extraction and purification after ultracentrifugation of infected cell supernatants. As the WNV genome 5′ and 3′ nontranslated regions (NTR) contain dsRNA loop structures that might confer RLR recognition, we also prepared *in vitro*-transcribed RNA fragments of the 5′ and 3′ NTR of the viral genome RNA. Each RNA preparation was transfected into WT MEFs in the presence of cycloheximide to prevent translation and *de novo* viral transcription, thus allowing us to assess the ability of the input RNA to stimulate innate immune signaling of IFN-β mRNA expression. Notably, transfection of icRNA significantly induced IFN-β mRNA expression in recipient cells compared to control cells transfected with mcRNA (1,050-fold [$P < 1 \times 10^{-5}$]) (Fig. 4b). We treated icRNA with Antarctic phosphatase (AP) to remove 3′ and 5′ phosphate moieties or with RNase III to digest dsRNA. In parallel, we recovered icRNA from WNV-infected $RNaseL^{-/-}$ cells, allowing us to assess innate immune signaling induced by possible RNA products of RNase L cleavage (56). icRNA stimulation of innate immune signaling was reduced by ~50% following phosphatase treatment, and it was completely ablated following RNase III treatment (1,050-fold versus 550-fold [$P < 0.001$]) (Fig. 4b). icRNA recovered from $RNaseL^{-/-}$ MEFs contained ~8 times more WNV RNA (data not shown); consequently, we adjusted the amount of input icRNA into recipient cells to equalize input RNA levels based on WNV genome equivalents. icRNA from

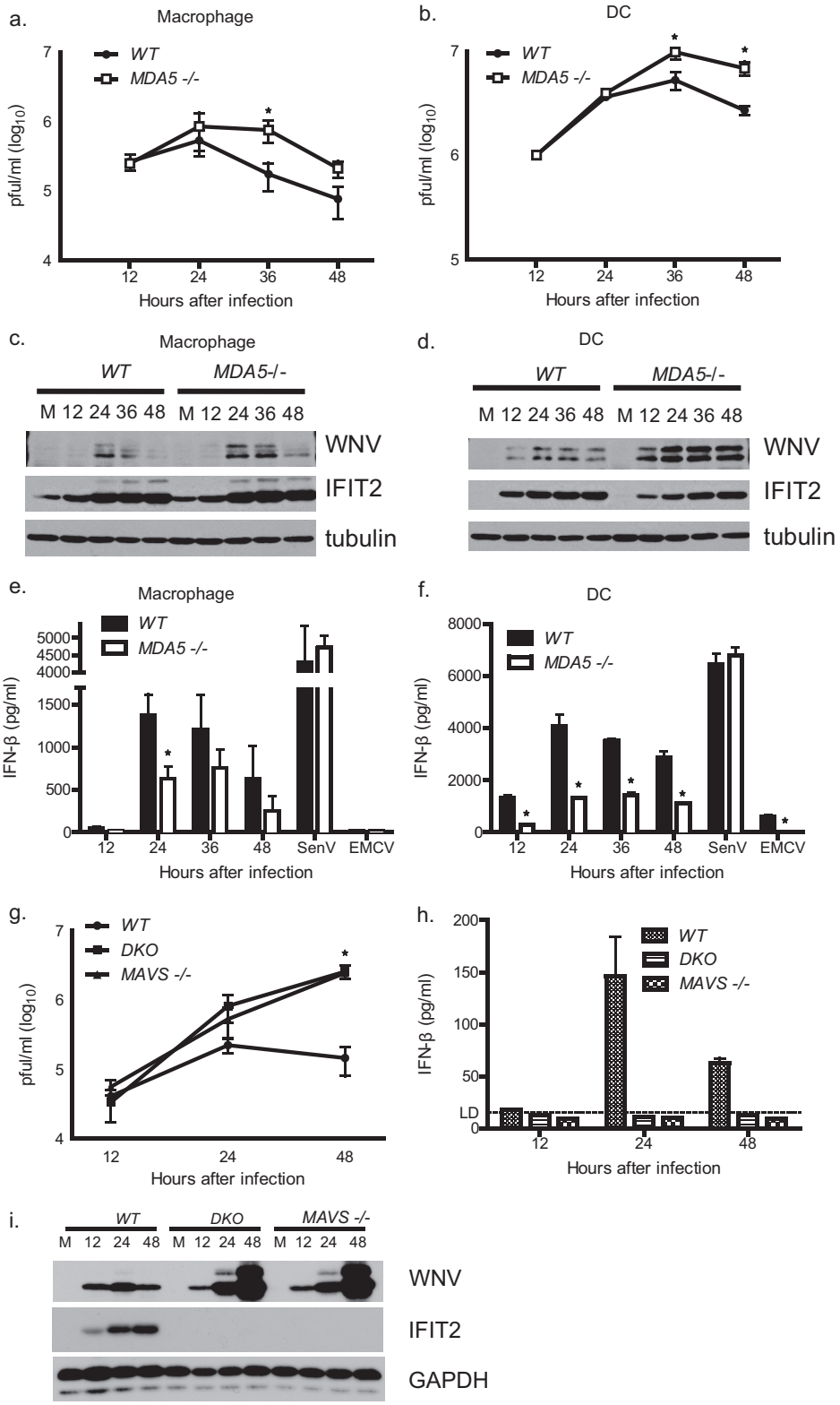

FIG 3 MDA5 is essential for viral replication control and innate immune induction in primary myeloid cells. Primary bone-marrow derived Mϕ and DCs were generated from control and RLR KO mice and infected with WNV. Supernatants and cellular protein lysates were collected over a time course to analyze viral replication and innate immune gene induction. (a and b) Supernatants from infected Mϕ and DCs were assayed for viral load by PFU assay. (c and d) Immunoblot analysis of protein abundance of WNV, IFIT2, and tubulin (control) in Mϕ and DCs. (e and f) IFN-β ELISA from WNV-infected cells or cells infected with Sendai virus or ECMV. (g to i) DCs generated from WT, *RIG-I*$^{-/-}$ × *MDA5*$^{-/-}$, or *MAVS*$^{-/-}$ mice and analyzed for viral load, protein abundance, and IFN-β protein production. Graphs show the means ± SDs from three independent experiments. *, $P < 0.05$.

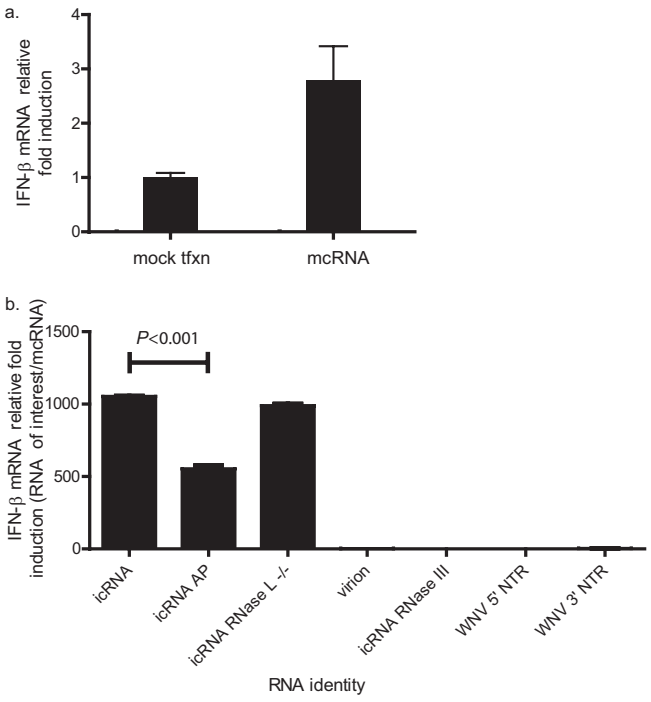

FIG 4 PAMP properties of WNV infection. (a) WT MEFs were transfected with reagent alone (mock tfxn) or with RNA isolated from uninfected cells (mcRNA). IFN-β mRNA was measured by qRT-PCR analysis and is shown relative to GAPDH. (b) RNA purified from cells infected with WNV for 24 h (icRNA), differentially modified icRNA (phosphatase-treated or RNase III-digested), *in vitro*-transcribed WNV RNA NTR motifs, and native virion RNA were purified, and equal mass quantities were transfected into WT MEFs in the presence of CHX. Innate immune gene induction was measured by qRT-PCR analysis for IFN-β mRNA, and relative fold induction normalized to GAPDH was determined compared to cells transfected with mock-infected cell RNA (mcRNA). Results are representative of three independent experiments.

RNaseL$^{-/-}$ cells induced levels of innate immune signaling comparable to those induced by icRNA recovered from WT cells. These results suggest that the WNV stimulatory PAMPs are generated independently of RNase L cleavage products. Neither vRNA nor the *in vitro*-transcribed viral NTR RNA induced appreciable levels of IFN-β compared to icRNA. This outcome was despite the presence of a 5′-ppp on the viral NTR RNA and the fact that larger copy number of viral RNA was transfected into cells from the NTR RNA compared to icRNA because equivalent mass quantities of RNA were transfected into cells for each condition. Despite an absence of innate immune signaling induction, there were in fact >470-fold more WNV genomes transfected from the vRNA than from icRNA, as determined by qRT-PCR (Fig. 4b). Thus, icRNA but not WNV virion RNA or viral 5′ppp-NTR RNA motifs induce innate immune signaling. These results imply that RLR PAMPs are not carried within the incoming WNV genome RNA of the virion but instead are produced within infected cells, and that PAMP recognition of icRNA by the RLRs includes RNA components with phosphate moieties and dsRNA motifs.

Differential kinetics of RIG-I and MDA5 PAMP production in WNV-infected cells. To determine how RIG-I and MDA5 individually contribute to the recognition of icRNA PAMPs, we examined icRNA signaling of innate immune genes in WT, *RIG-I*$^{-/-}$, and *MDA5*$^{-/-}$ MEFs. We isolated mcRNA from WT mock-infected cells and icRNA from WNV-infected cells at 6, 10, 12, and 34 h after infection. Equal mass amounts of the recovered icRNA or mcRNA were transfected into WT, *RIG-I*$^{-/-}$, and *MDA5*$^{-/-}$ cells in the presence of cycloheximide, and IFN-β mRNA levels were measured by qRT-PCR. icRNA recovered after 6 h postinfection stimulated IFN-β mRNA induction in WT cells, but this response was reduced in both *RIG-I*$^{-/-}$ and *MDA5*$^{-/-}$ cells (Fig. 5a). We observed a difference in early signaling between *RIG-I*$^{-/-}$ and *MDA5*$^{-/-}$ cells in response to icRNA harvested at 10 and 12 h after infection but not at 34 h after infection. As shown in Fig. 5a, the early signaling of IFN-β mRNA induction was impaired in *RIG-I*$^{-/-}$ cells in which signaling was mediated exclusively by MDA5. Signaling was comparable in both *RIG-I*$^{-/-}$ and *MDA5*$^{-/-}$ cells upon transfection of icRNA recovered from later times (34 h) postinfection. Thus, icRNA from early time points of WNV infection contains PAMPs that were sensed preferentially by RIG-I, whereas icRNA from later time points of infection contains PAMPs that were detected by both RIG-I and MDA5.

As phosphatase treatment of 24 h-derived icRNA reduced PAMP stimulation by ~50% (see Fig. 4b), we next assessed the requirement for RNA phosphate moieties to affect PAMP sensing by either RIG-I or MDA5. icRNA was recovered from cells 24 h after WNV infection and treated with phosphatase prior to transfection of WT, *RIG-I*$^{-/-}$, or *MDA5*$^{-/-}$ MEFs. Phosphatase treatment of icRNA had a minimal effect on reducing IFN-β signaling in *RIG-I*$^{-/-}$ MEFs, suggesting that the remaining MDA5 sensing of the WNV PAMP was not affected by loss of exposed phosphates on PAMP RNA. In contrast, phosphatase treatment of icRNA caused an almost complete loss of innate immune signaling in *MDA5*$^{-/-}$ MEFs such that less than 10% signaling remained compared to that observed for untreated icRNA transfected into *MDA5*$^{-/-}$ MEFs (Fig. 5b). As a control, these RNAs also were transfected into DKO and *MAVS*$^{-/-}$ cells; we failed to see significant signaling in either cell type (Fig. 5b). These results reveal a temporal distribution of PAMP detection by RIG-I and MDA5 during WNV infection. Recognition of PAMP RNA within WNV-infected cells at early times occurs in a RIG-I-predominant manner that depends on exposed phosphate moieties, whereas at later times PAMP recognition is performed cooperatively by RIG-I and MDA5. Additionally, our results suggest that WNV generates RIG-I and MDA5-specific PAMPs with differential kinetics over the course of viral replication, and that both PAMPs feature a component of dsRNA that imparts RLR recognition. Results from these RNA transfection experiments agree with infection data (Fig. 2) showing that the loss of RIG-I and MDA5 or MAVS abolishes innate immune signaling in response to cytosolic RNA.

DISCUSSION

The central role of MAVS-dependent signaling in controlling WNV infection and pathogenesis has been established and implicates an essential role for RLRs in immunity against WNV (12, 14, 29, 47). Herein, we delineated the role of RIG-I and MDA5 as individual PRRs in contributing to the control of WNV and induction of innate immune genes *in vitro* and *in vivo*. We found that each PRR is essential for full immune protection against WNV. In addition, the susceptibility of mice to WNV infection lacking both PRRs recapitulates the phenotype of *MAVS*$^{-/-}$ mice, confirming the essential nature of RLR signaling over other innate immune induction pathways (14). The susceptibility phenotype in DKO mice occurred despite a full complement and expression

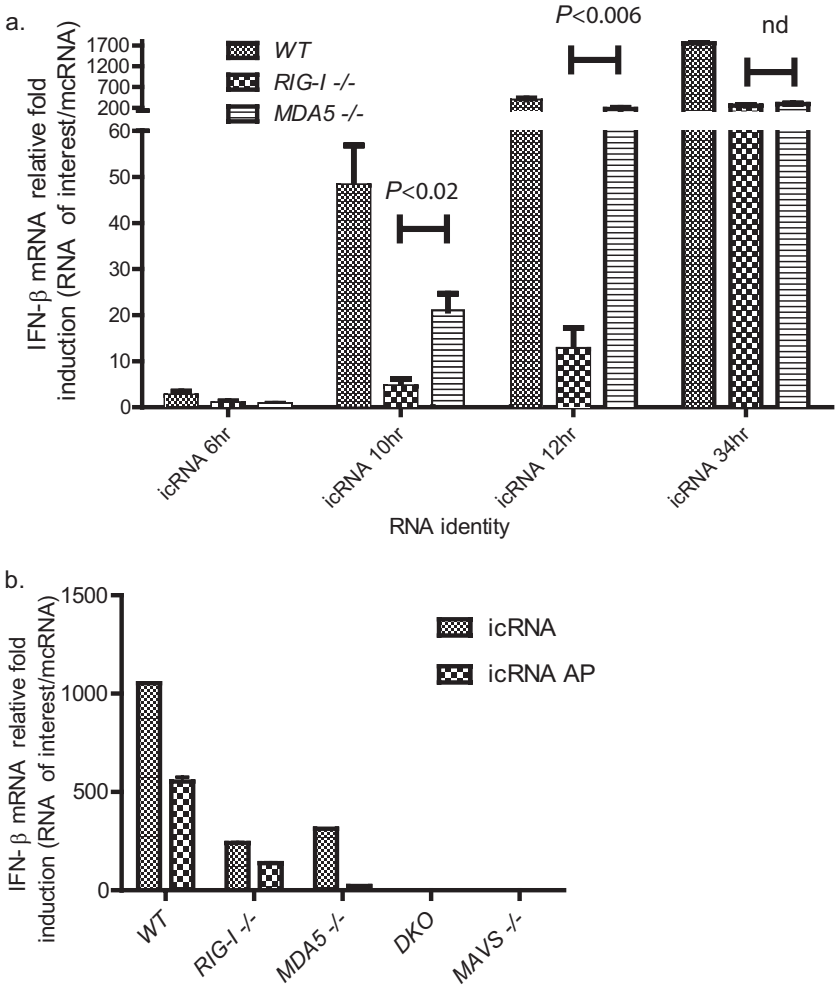

FIG 5 Distinct RIG-I and MDA5-dependent PAMPs accumulate with differential kinetics during WNV infection. (a) icRNA was isolated from WT cells infected with WNV after 6, 10, 12, and 34 h of infection and subsequently transfected into WT, *RIG-I*$^{-/-}$, or *MDA5*$^{-/-}$ MEFs in the presence of CHX. Innate immune gene induction was measured by qRT-PCR analysis for IFN-β mRNA, and relative fold induction after normalization to GAPDH was compared to that of cells transfected mcRNA. icRNA induced less IFN-β mRNA at all time points in RLR-deficient recipient MEFs, but significantly less IFN-β mRNA only was induced in *RIG-I*$^{-/-}$ MEFs from icRNA collected at 10 and 12 hpi ($P < 0.02$ and $P < 0.006$, respectively). nd, no difference. (b) icRNA from 24 hpi was treated with phosphatase and transfected into WT, *RIG-I*$^{-/-}$, and *MDA5*$^{-/-}$ MEFs in the presence of CHX, and IFN-β mRNA induction was measured. Results are representative of three independent experiments.

of TLRs and NOD-like receptors (NLRs) in these mice. Thus, RIG-I and MDA5 are essential PRRs of WNV recognition, with each serving to transduce innate immune signaling through MAVS in response to infection of key target cells. The loss of RIG-I or MDA5 can be compensated partially by the other, but loss of both genes results in a severe loss of innate immunity to infection.

During an extensive time course infection of MEFs, we observed a deficit in innate immune signaling at early time points in *RIG-I*$^{-/-}$ cells. This observation is consistent with our finding that viral PAMPs from early time points after WNV infection are preferentially sensed by RIG-I. Additionally, we demonstrated that the WNV PAMP recognized by RIG-I is almost completely dependent on phosphate moieties and dsRNA structure, whereas the MDA5 PAMP is largely independent of phosphate moieties but dependent on dsRNA structure. Prior studies have suggested that multiple regions of the WNV RNA present within both genome and antigenome replication intermediates can be recognized by RIG-I as PAMP motifs (32). We too observed a modest innate immune gene induction following transfection of an *in vitro*-transcribed WNV 5′ NTR RNA (3-fold), but this stimulation was marginal compared to the PAMPs present in RNA generated in WNV-infected cells (icRNA; >1,000-fold induction of IFN-β mRNA expression). The low level of innate immune stimulation by *in vitro*-transcribed WNV RNA sequences containing highly structured motifs and 5′-ppp, coupled with the reduction of signaling observed from phosphatase-treated icRNA, indicates that WNV PAMPs of RIG-I recognition are comprised of multiple motifs. In this case, 5′-ppp is a component of this recognition that may also include specific sequence composition and certain RNA structures (35). Such a 5′-ppp PAMP unit would be present on viral RNA during virus replication but is not associated within the incoming virion RNA, due to the absence of negative-strand RNA and presence of a 5′ type 1 cap on the genomic RNA, which effectively blocks 5′-ppp recognition by RIG-I.

For MDA5, our observations reveal a strict dependence on dsRNA for signaling by icRNA. Moreover, our data indicate that

MDA5 contributes to innate immune induction at later times after initial WNV infection. This response leads to an amplification of innate immune signaling to IFN-β, as well as response diversification due to the induced expression (and activation) of IRF-7 and other innate immune signal transducers to drive the expression of IFN-α2a and increased ISG and cytokine expression (17, 50). Consistent with this, collaborative studies reveal that MDA5 is essential for the optimal priming of effector T cells and that this process occurs in a T cell-nonautonomous manner, with MDA5 function required for the priming environment (48). Thus, PAMP recognition and signaling by MDA5, as WNV replication proceeds, mediate an innate immune response that restricts viral infection and produces mediators supporting T cell priming, which links innate to adaptive immunity through RLR signaling.

Our study supports a model in which capped, incoming WNV RNA genomes are hidden from RLR detection, yet during viral RNA replication the accumulation of uncapped genomes with exposed phosphate moieties and secondary structure are initially sensed by RIG-I. It remains a possibility that cleavage of viral or endogenous RNA by cellular enzymes may contribute to or amplify PAMP generation, though our results suggest that intact icRNA is likely the dominant source of stimulatory RNA. In this respect, we note that as icRNA contains both viral and cellular RNA, the latter might contribute to RLR signaling if specific PAMP motifs are generated and displayed. One scenario would involve RLR recognition of virus-induced cellular RNA species that can serve as endogenous PAMPs of innate immune signaling.

Efficient and early PAMP recognition is required to induce an IRF-3-dependent gene expression signature that controls viral replication in a cell-intrinsic manner (16). In cells lacking RIG-I expression, WNV replication proceeds at a higher rate. In contrast, in *MDA5*$^{-/-}$ MEFs, a deficit of innate immune signaling amplification and diversification is marked by a deficiency in IRF-7-driven IFN-α2a expression without an increase in viral replication. This phenotype is consistent with experiments in *MDA5*$^{-/-}$ neurons (48) and may reflect the ability of pathogenic WNV to block type I IFN signaling at later times in infection when MDA5 PAMPs accumulate (17, 53, 54). It has recently been proposed that the signaling-active form is a large MDA5 oligomer bound to RNA (57). In the context of WNV, MDA5 might require long dsRNA replication intermediates for such oligomer assembly, which accumulate at later times when replication peaks.

In summary, our observations define the complementary and individual roles of RIG-I and MDA5 in detection and control of WNV infection. While each RLR can recognize WNV independently, signaling by both optimally restricts flavivirus infection and protects against disease pathogenesis.

ACKNOWLEDGMENTS

This work was supported by National Institutes of Health grants U19 AI083019 and RO1 AI104002.

We also thank Maggie Brassil and Gabrielle Blahnik for technical assistance.

REFERENCES

1. **Campbell GL, Marfin AA, Lanciotti RS, Gubler DJ.** 2002. West Nile virus. Lancet Infect. Dis. **2:**519–529.
2. **Centers for Disease Control and Prevention.** 2011. West Nile virus disease and other arboviral diseases—United States, 2010. MMWR Morb. Mortal. Wkly. Rep. **60:**1009–1013.
3. **Centers for Disease Control and Prevention.** 2013. West Nile virus: final cumulative maps and data for 1999–2012. Centers for Disease Control and Prevention, Atlanta, GA. http://www.cdc.gov/westnile/statsMaps/cumMapsData.html.
4. **Papa A, Xanthopoulou K, Gewehr S, Mourelatos S.** 2011. Detection of West Nile virus lineage 2 in mosquitoes during a human outbreak in Greece. Clin. Microbiol. Infect. **17:**1176–1180.
5. **Savini G, Capelli G, Monaco F, Polci A, Russo F, Di Gennaro A, Marini V, Teodori L, Montarsi F, Pinoni C, Pisciella M, Terregino C, Marangon S, Capua I, Lelli R.** 2012. Evidence of West Nile virus lineage 2 circulation in Northern Italy. Vet. Microbiol. **158:**267–273.
6. **Hayes EB, Komar N, Nasci RS, Montgomery SP, O'Leary DR, Campbell GL.** 2005. Epidemiology and transmission dynamics of West Nile virus disease. Emerg. Infect. Dis. **11:**1167–1173.
7. **Samuel MA, Diamond MS.** 2006. Pathogenesis of West Nile Virus infection: a balance between virulence, innate and adaptive immunity, and viral evasion. J. Virol. **80:**9349–9360.
8. **Petersen LR, Hayes EB.** 2004. Westward ho? The spread of West Nile virus. N. Engl. J. Med. **351:**2257–2259.
9. **Lim PY, Behr MJ, Chadwick CM, Shi PY, Bernard KA.** 2011. Keratinocytes are cell targets of West Nile virus in vivo. J. Virol. **85:**5197–5201.
10. **Suthar MS, Diamond MS, Gale M, Jr.** 2013. West Nile virus infection and immunity. Nat. Rev. Microbiol. **11:**115–128.
11. **Daffis S, Samuel MA, Suthar MS, Gale M, Jr, Diamond MS.** 2008. Toll-like receptor 3 has a protective role against West Nile virus infection. J. Virol. **82:**10349–10358.
12. **Fredericksen BL, Keller BC, Fornek J, Katze MG, Gale M, Jr.** 2008. Establishment and maintenance of the innate antiviral response to West Nile virus involves both RIG-I and MDA5 signaling through IPS-1. J. Virol. **82:**609–616.
13. **Fredericksen BL, Smith M, Katze MG, Shi PY, Gale M, Jr.** 2004. The host response to West Nile virus infection limits viral spread through the activation of the interferon regulatory factor 3 pathway. J. Virol. **78:**7737–7747.
14. **Suthar MS, Ma DY, Thomas S, Lund JM, Zhang N, Daffis S, Rudensky AY, Bevan MJ, Clark EA, Kaja MK, Diamond MS, Gale M, Jr.** 2010. IPS-1 is essential for the control of West Nile virus infection and immunity. PLoS Pathog. **6:**e1000757. doi:10.1371/journal.ppat.1000757.
15. **Samuel MA, Whitby K, Keller BC, Marri A, Barchet W, Williams BR, Silverman RH, Gale M, Jr, Diamond MS.** 2006. PKR and RNase L contribute to protection against lethal West Nile virus infection by controlling early viral spread in the periphery and replication in neurons. J. Virol. **80:**7009–7019.
16. **Daffis S, Samuel MA, Keller BC, Gale M, Jr, Diamond MS.** 2007. Cell-specific IRF-3 responses protect against West Nile virus infection by interferon-dependent and -independent mechanisms. PLoS Pathog. **3:**e106. doi:10.1371/journal.ppat.0030106.
17. **Daffis S, Samuel MA, Suthar MS, Keller BC, Gale M, Jr, Diamond MS.** 2008. Interferon regulatory factor IRF-7 induces the antiviral alpha interferon response and protects against lethal West Nile virus infection. J. Virol. **82:**8465–8475.
18. **Samuel MA, Diamond MS.** 2005. Alpha/beta interferon protects against lethal West Nile virus infection by restricting cellular tropism and enhancing neuronal survival. J. Virol. **79:**13350–13361.
19. **Glass WG, Lim JK, Cholera R, Pletnev AG, Gao JL, Murphy PM.** 2005. Chemokine receptor CCR5 promotes leukocyte trafficking to the brain and survival in West Nile virus infection. J. Exp. Med. **202:**1087–1098.
20. **Diamond MS, Shrestha B, Marri A, Mahan D, Engle M.** 2003. B cells and antibody play critical roles in the immediate defense of disseminated infection by West Nile encephalitis virus. J. Virol. **77:**2578–2586.
21. **Shrestha B, Diamond MS.** 2004. Role of CD8+ T cells in control of West Nile virus infection. J. Virol. **78:**8312–8321.
22. **Sitati EM, Diamond MS.** 2006. CD4+ T-cell responses are required for clearance of West Nile virus from the central nervous system. J. Virol. **80:**12060–12069.
23. **Cho H, Proll SC, Szretter KJ, Katze MG, Gale M, Jr, Diamond MS.** 2013. Differential innate immune response programs in neuronal subtypes determine susceptibility to infection in the brain by positive-stranded RNA viruses. Nat. Med. **19:**458–464.
24. **Suthar MS, Brassil MM, Blahnik G, McMillan A, Ramos HJ, Proll SC, Belisle SE, Katze MG, Gale M, Jr.** 2013. A systems biology approach reveals that tissue tropism to West Nile virus is regulated by antiviral genes and innate immune cellular processes. PLoS Pathog. **9:**e1003168. doi:10.1371/journal.ppat.1003168.

25. **Loo YM, Gale M, Jr.** 2011. Immune signaling by RIG-I-like receptors. Immunity **34:**680–692.
26. **Loo YM, Fornek J, Crochet N, Bajwa G, Perwitasari O, Martinez-Sobrido L, Akira S, Gill MA, Garcia-Sastre A, Katze MG, Gale M, Jr.** 2008. Distinct RIG-I and MDA5 signaling by RNA viruses in innate immunity. J. Virol. **82:**335–345.
27. **Daffis S, Suthar MS, Szretter KJ, Gale M, Jr, Diamond MS.** 2009. Induction of IFN-beta and the innate antiviral response in myeloid cells occurs through an IPS-1-dependent signal that does not require IRF-3 and IRF-7. PLoS Pathog. **5:**e1000607. doi:10.1371/journal.ppat.1000607.
28. **Fredericksen BL, Gale M, Jr.** 2006. West Nile virus evades activation of interferon regulatory factor 3 through RIG-I-dependent and -independent pathways without antagonizing host defense signaling. J. Virol. **80:**2913–2923.
29. **Lazear HM, Lancaster A, Wilkins C, Suthar MS, Huang A, Vick SC, Clepper L, Thackray L, Brassil MM, Virgin HW, Nikolich-Zugich J, Moses AV, Gale M, Jr, Fruh K, Diamond MS.** 2013. IRF-3, IRF-5, and IRF-7 coordinately regulate the type I IFN response in myeloid dendritic cells downstream of MAVS signaling. PLoS Pathog. **9:**e1003118. doi:10.1371/journal.ppat.1003118.
30. **Meylan E, Curran J, Hofmann K, Moradpour D, Binder M, Bartenschlager R, Tschopp J.** 2005. Cardif is an adaptor protein in the RIG-I antiviral pathway and is targeted by hepatitis C virus. Nature **437:**1167–1172.
31. **Paz S, Sun Q, Nakhaei P, Romieu-Mourez R, Goubau D, Julkunen I, Lin R, Hiscott J.** 2006. Induction of IRF-3 and IRF-7 phosphorylation following activation of the RIG-I pathway. Cell. Mol. Biol. (Noisy-le-grand) **52:**17–28.
32. **Shipley JG, Vandergaast R, Deng L, Mariuzza RA, Fredericksen BL.** 2012. Identification of multiple RIG-I-specific pathogen associated molecular patterns within the West Nile virus genome and antigenome. Virology **432:**232–238.
33. **Hornung V, Ellegast J, Kim S, Brzozka K, Jung A, Kato H, Poeck H, Akira S, Conzelmann KK, Schlee M, Endres S, Hartmann G.** 2006. 5′-Triphosphate RNA is the ligand for RIG-I. Science **314:**994–997.
34. **Marques JT, Devosse T, Wang D, Zamanian-Daryoush M, Serbinowski P, Hartmann R, Fujita T, Behlke MA, Williams BR.** 2006. A structural basis for discriminating between self and nonself double-stranded RNAs in mammalian cells. Nat. Biotechnol. **24:**559–565.
35. **Saito T, Owen DM, Jiang F, Marcotrigiano J, Gale M, Jr.** 2008. Innate immunity induced by composition-dependent RIG-I recognition of hepatitis C virus RNA. Nature **454:**523–527.
36. **Schlee M, Roth A, Hornung V, Hagmann CA, Wimmenauer V, Barchet W, Coch C, Janke M, Mihailovic A, Wardle G, Juranek S, Kato H, Kawai T, Poeck H, Fitzgerald KA, Takeuchi O, Akira S, Tuschl T, Latz E, Ludwig J, Hartmann G.** 2009. Recognition of 5′ triphosphate by RIG-I helicase requires short blunt double-stranded RNA as contained in panhandle of negative-strand virus. Immunity **31:**25–34.
37. **Pichlmair A, Schulz O, Tan CP, Naslund TI, Liljestrom P, Weber F, Reis e Sousa C.** 2006. RIG-I-mediated antiviral responses to single-stranded RNA bearing 5′-phosphates. Science **314:**997–1001.
38. **Kato H, Takeuchi O, Mikamo-Satoh E, Hirai R, Kawai T, Matsushita K, Hiiragi A, Dermody TS, Fujita T, Akira S.** 2008. Length-dependent recognition of double-stranded ribonucleic acids by retinoic acid-inducible gene-I and melanoma differentiation-associated gene 5. J. Exp. Med. **205:**1601–1610.
39. **Pichlmair A, Schulz O, Tan CP, Rehwinkel J, Kato H, Takeuchi O, Akira S, Way M, Schiavo G, Reis e Sousa C.** 2009. Activation of MDA5 requires higher-order RNA structures generated during virus infection. J. Virol. **83:**10761–10769.
40. **Pijlman GP, Funk A, Kondratieva N, Leung J, Torres S, van der Aa L, Liu WJ, Palmenberg AC, Shi PY, Hall RA, Khromykh AA.** 2008. A highly structured, nuclease-resistant, noncoding RNA produced by flaviviruses is required for pathogenicity. Cell Host Microbe **4:**579–591.
41. **Gillespie LK, Hoenen A, Morgan G, Mackenzie JM.** 2010. The endoplasmic reticulum provides the membrane platform for biogenesis of the flavivirus replication complex. J. Virol. **84:**10438–10447.
42. **Hoenen A, Liu W, Kochs G, Khromykh AA, Mackenzie JM.** 2007. West Nile virus-induced cytoplasmic membrane structures provide partial protection against the interferon-induced antiviral MxA protein. J. Gen. Virol. **88:**3013–3017.
43. **Lindenbach BDR, CM.** 2001. Flaviviridae: the viruses and their replication, p 991–1041. *In* Knipe DM, Howley PM, Griffin DE, Lamb RA, Martin MA, Roizman B, Straus SE (ed), Fields virology, 4th ed, vol 1. Lippincott Williams and Wilkins, Philadelphia, PA.
44. **Kato H, Takeuchi O, Sato S, Yoneyama M, Yamamoto M, Matsui K, Uematsu S, Jung A, Kawai T, Ishii KJ, Yamaguchi O, Otsu K, Tsujimura T, Koh CS, Reis e Sousa C, Matsuura Y, Fujita T, Akira S.** 2006. Differential roles of MDA5 and RIG-I helicases in the recognition of RNA viruses. Nature **441:**101–105.
45. **Querec TD, Akondy RS, Lee EK, Cao W, Nakaya HI, Teuwen D, Pirani A, Gernert K, Deng J, Marzolf B, Kennedy K, Wu H, Bennouna S, Oluoch H, Miller J, Vencio RZ, Mulligan M, Aderem A, Ahmed R, Pulendran B.** 2009. Systems biology approach predicts immunogenicity of the yellow fever vaccine in humans. Nat. Immunol. **10:**116–125.
46. **Kawai T, Takahashi K, Sato S, Coban C, Kumar H, Kato H, Ishii KJ, Takeuchi O, Akira S.** 2005. IPS-1, an adaptor triggering RIG-I- and Mda5-mediated type I interferon induction. Nat. Immunol. **6:**981–988.
47. **Suthar MS, Ramos HJ, Brassil MM, Netland J, Chappell CP, Blahnik G, McMillan A, Diamond MS, Clark EA, Bevan MJ, Gale M, Jr.** 2012. The RIG-I-like receptor LGP2 controls CD8(+) T cell survival and fitness. Immunity **37:**235–248.
48. **Lazear HM, Pinto AK, Ramos HJ, Vick SC, Shrestha B, Suthar MS, Gale M, Jr, Diamond MS.** 2013. Pattern recognition receptor MDA5 modulates $CD8^+$ T cell-dependent clearance of West Nile virus from the central nervous system. J. Virol. **87:**11401–11415.
49. **Dong H, Ren S, Zhang B, Zhou Y, Puig-Basagoiti F, Li H, Shi PY.** 2008. West Nile virus methyltransferase catalyzes two methylations of the viral RNA cap through a substrate-repositioning mechanism. J. Virol. **82:**4295–4307.
50. **Perwitasari O, Cho H, Diamond MS, Gale M, Jr.** 2011. Inhibitor of kappaB kinase epsilon (IKK(epsilon)), STAT1, and IFIT2 proteins define novel innate immune effector pathway against West Nile virus infection. J. Biol. Chem. **286:**44412–44423.
51. **Gitlin L, Barchet W, Gilfillan S, Cella M, Beutler B, Flavell RA, Diamond MS, Colonna M.** 2006. Essential role of mda-5 in type I IFN responses to polyriboinosinic:polyribocytidylic acid and encephalomyocarditis picornavirus. Proc. Natl. Acad. Sci. U. S. A. **103:**8459–8464.
52. **Sato M, Suemori H, Hata N, Asagiri M, Ogasawara K, Nakao K, Nakaya T, Katsuki M, Noguchi S, Tanaka N, Taniguchi T.** 2000. Distinct and essential roles of transcription factors IRF-3 and IRF-7 in response to viruses for IFN-alpha/beta gene induction. Immunity **13:**539–548.
53. **Keller BC, Fredericksen BL, Samuel MA, Mock RE, Mason PW, Diamond MS, Gale M, Jr.** 2006. Resistance to alpha/beta interferon is a determinant of West Nile virus replication fitness and virulence. J. Virol. **80:**9424–9434.
54. **Laurent-Rolle M, Boer EF, Lubick KJ, Wolfinbarger JB, Carmody AB, Rockx B, Liu W, Ashour J, Shupert WL, Holbrook MR, Barrett AD, Mason PW, Bloom ME, Garcia-Sastre A, Khromykh AA, Best SM.** 2010. The NS5 protein of the virulent West Nile virus NY99 strain is a potent antagonist of type I interferon-mediated JAK-STAT signaling. J. Virol. **84:**3503–3515.
55. **Daffis S, Szretter KJ, Schriewer J, Li J, Youn S, Errett J, Lin TY, Schneller S, Zust R, Dong H, Thiel V, Sen GC, Fensterl V, Klimstra WB, Pierson TC, Buller RM, Gale M, Jr., Shi PY, Diamond MS.**2010. 2′-O methylation of the viral mRNA cap evades host restriction by IFIT family members. Nature **468:**452–456.
56. **Malathi K, Dong B, Gale M, Jr, Silverman RH.** 2007. Small self-RNA generated by RNase L amplifies antiviral innate immunity. Nature **448:**816–819.
57. **Berke IC, Modis Y.** 2012. MDA5 cooperatively forms dimers and ATP-sensitive filaments upon binding double-stranded RNA. EMBO J. **31:**1714–1726.